First Observation of the Charmless Baryonic Decay $B^+ \to \bar{\Lambda} p \bar{p} p$

R. Aaij *et al.*[*]
(LHCb Collaboration)

(Received 25 August 2025; accepted 25 November 2025; published 22 December 2025)

A search for the charmless baryonic decay $B^+ \to \bar{\Lambda} p \bar{p} p$ is performed using proton-proton collision data recorded by the LHCb experiment, corresponding to an integrated luminosity of 5.4 fb^{-1}. The branching fraction for this decay is measured for the first time relative to that of the topologically similar decay $B^+ \to J/\psi K^+$, with $J/\psi \to \bar{\Lambda} p K^-$. The branching fraction is measured to be $\mathcal{B}(B^+ \to \bar{\Lambda} p \bar{p} p) = (2.15 \pm 0.35 \pm 0.12 \pm 0.28) \times 10^{-7}$, where the first uncertainty is statistical, the second is systematic, and the third arises from the uncertainty in the normalization channel branching fraction. The CP asymmetry is measured to be $\mathcal{A}_{CP} = (5.4 \pm 15.6 \pm 2.4)\%$, where the uncertainties are statistical and systematic. The background-subtracted invariant-mass distributions of $\bar{\Lambda} p$ and $\bar{p} p$ pairs exhibit pronounced enhancements at both kinematic thresholds, in contrast to a uniform phase-space distribution.

DOI: 10.1103/3pcs-dxtn

Studies of exclusive B-meson decays to final states containing both baryons and mesons have been ongoing since the late 1980s [1]. Several baryonic B decay modes have been observed, including three-body final states such as $p\bar{p}K^+$, $p\bar{p}\pi^+$, $p\bar{p}K^0_S$, and $p\bar{p}K^*(892)^+$ [2,3], as well as four-body modes like $p\bar{p}\pi^+\pi^-$ and $p\bar{p}K^+K^-$ [4]. In the standard model, these decays proceed via $b \to u$ tree-level and $b \to s(d)$ electroweak penguin diagrams, providing a valuable laboratory for studying direct CP violation and testing hadronic models [5,6].

Unlike mesonic modes, baryonic B decays exhibit a unique feature known as threshold enhancement: a pronounced peak near the invariant-mass threshold of the baryon-antibaryon pair [2,3]. Final states with two baryon-antibaryon pairs are particularly intriguing, as they probe hadronization dynamics beyond those accessible with a single pair [7].

The LHCb Collaboration recently reported the first observation of a four-body charmless fully baryonic weak decay, $B^0 \to p\bar{p}p\bar{p}$ [8], which mainly proceeds via a $b \to u$ tree-level internal W-boson emission [7]. The measured branching fraction, $\mathcal{B}(B^0 \to p\bar{p}p\bar{p}) = (2.2 \pm 0.4 \pm 0.1 \pm 0.1) \times 10^{-8}$, is approximately 2 orders of magnitude lower than those of analogous four-body baryonic B decays, such as $B^0 \to p\bar{p}\pi^+\pi^-$ [4]. To explain the overall observed suppression, form factors that describe the evolution of short-distance systems to those with baryons in the final state have been proposed [7]. In this approach, a *double-enhancement* mechanism in baryon-pair formation was also proposed. It increases the decay rate in the limited regions of phase space where one or both baryon pairs are produced near threshold. With this effect, the decay $B^+ \to \bar{\Lambda} p \bar{p} p$ (The inclusion of charge-conjugate processes is implied throughout, except in the discussion of asymmetries.), which proceeds via a combination of via a combination of $b \to u$ tree level suppressed by Cabibbo-Kobayashi-Maskawa (CKM) matrix elements and $b \to s$ electroweak loop amplitudes, is expected to have a branching fraction of $\mathcal{B}(B^+ \to \bar{\Lambda} p \bar{p} p) = (7.4^{+0.6}_{-0.2} \pm 0.03^{+3.6}_{-2.6}) \times 10^{-7}$ [7], where the uncertainty arises from nonfactorizable QCD corrections, the CKM matrix-element inputs, and form-factor modeling. The comparatively large branching fraction of this decay offers a promising opportunity to study the mass spectra of baryon pairs and explore baryon-pair formation mechanisms. The mass spectra may reveal resonant structures such as the $X(1835)$ and $X(2085)$, which are interpreted as baryonium-like bound states [9,10]. In addition, owing to the interference between tree-level and penguin diagrams in the low $m(\bar{\Lambda} p)$ and $m(\bar{p} p)$ mass regions, sizeable direct CP asymmetries are possible [11].

In this Letter, the $B^+ \to \bar{\Lambda} p \bar{p} p$ decay is studied using proton-proton (pp) collision data collected by the LHCb experiment over the period 2016–2018 at a center-of-mass energy $\sqrt{s} = 13$ TeV and corresponding to an integrated luminosity of approximately 5.4 fb^{-1}. The branching fraction of the signal decay is measured relative to that of the topologically similar normalization mode, $B^+ \to J/\psi(\to \bar{\Lambda} p K^-) K^+$, using a simultaneous fit across all data-taking periods. In addition, this Letter presents a study of the $m(\bar{\Lambda} p)$ and

[*]Full author list given at the end of the Letter.

$m(\bar{p}p)$ spectra and CP asymmetry in a purely baryonic four-body decay.

The LHCb detector [12,13] is a single-arm forward spectrometer covering the pseudorapidity range $2 < \eta < 5$, designed for the study of particles containing b or c quarks. The detector used for this analysis includes a high-precision tracking system consisting of a silicon-strip vertex detector (VELO) surrounding the pp interaction region [14], a large-area silicon-strip detector located upstream of a dipole magnet with a bending power of about 4 T m, and three stations of silicon-strip detectors and straw drift tubes [15] placed downstream of the magnet. The tracking system provides measurements of the track momentum and impact parameter (IP) and is used to reconstruct the primary pp interaction vertex (PV), where the IP is the shortest distance between the extrapolation of a track and a PV. Different types of charged hadrons are distinguished using particle identification (PID) information from two ring-imaging Cherenkov detectors [16]. The $\Lambda \to p\pi^-$ decay is reconstructed in two distinct categories depending on whether the decay products are reconstructed in all tracking detectors (*long*) or in all but the VELO (*downstream*). While candidates in the long category have better mass, momentum, and vertex resolution than those in the downstream category, the downstream category accounts for two-thirds of the total Λ yield.

Online event selection is performed by a trigger [17] that consists of a hardware stage, based on information from the calorimeter and muon systems, followed by a two-level software stage, which applies a full event reconstruction. At the hardware stage, events are required to have a muon with high transverse momentum (p_{T}) or a hadron, photon, or electron with high transverse energy in the calorimeters. The first-level software trigger requires one or two tracks that are likely to originate from B decays. The second-level software trigger requires a two-, three-, or four-track secondary vertex with a significant displacement from any PV. A multivariate algorithm [18] is to identify secondary vertices consistent with the decay of a b hadron.

Simulated samples are used to study the properties of the signal, normalization, and background channels. PYTHIA [19] generates pp collisions using an LHCb-specific configuration [20]. Decays of unstable particles are described by EvtGen [21], in which final-state radiation is generated using PHOTOS [22]. The interactions of generated particles with the detector material, and their responses, are implemented using the Geant4 toolkit [23,24], as described in Ref. [25]. Simulated signal and normalization decays are generated using phase-space models.

Off-line candidates are selected by exploiting the characteristic topology and kinematic features of four-body decays to final states containing a Λ baryon. The preselection requires loose track quality and applies minimal kinematic requirements to the Λ and B^+ candidates. All charged tracks except those used to reconstruct Λ candidates must originate from within the VELO and are required to have a good track-fit quality. Fake tracks, which are reconstructed from detector hits that do not correspond to real particles, are rejected by applying a selection on the fake-track probability [26]. A minimum p_{T} of 250, 200, and 400 MeV$/c$ is required for the proton, kaon, and Λ baryon, respectively. Each track must have a significant χ^2_{IP}, where χ^2_{IP} is defined as the difference between the vertex fit χ^2 of a PV reconstructed with and without the considered track. Candidate Λ baryons are formed by combining proton and pion track candidates that are fitted to a common decay vertex. A loose PID requirement on the proton from the Λ baryon is applied at this stage. For Λ candidates in the long category, the selection algorithm further requires that the decay vertices of the Λ baryon and the associated B^+ candidate are well separated. The Λ decay products must satisfy $|m(p\pi) - M_\Lambda| < 6$ MeV$/c^2$, where M_Λ is the known Λ mass [27]. Candidate B^+ mesons are reconstructed by combining a Λ candidate with three charged final-state particles into a common vertex. Both the $B^+ \to \bar{\Lambda}p\bar{p}p$ and the $B^+ \to J/\psi(\to \bar{\Lambda}pK^-)K^+$ decay chains are fitted constraining the Λ mass to its known value [27]. The PV that fits best to the flight direction of the B^+ candidate is taken as the associated PV. The angle between the B^+ momentum direction and the displacement vector from the PV to the B^+ decay vertex is required to be less than 2.5°. The B^+ candidate is also required to have $p_{\mathrm{T}} > 3000$ MeV$/c$ and a large decay length significance, defined as the χ^2 of the separation between the B^+ decay vertex and the associated PV, ensuring a clear displacement from the PV.

The final selection of B^+ candidates uses the two most powerful variables that discriminate between signal and background: χ^2_{IP} of the B^+ candidate, defined as the difference between the vertex fit χ^2 of a PV reconstructed with and without the B^+ meson, and the product of the nominal particle-identification classifiers of the three charged final-state particles, $\prod_i \mathcal{P}_i$. The χ^2_{IP} distribution for signal is approximately that of χ^2 for one degree of freedom. Each classifier, $\mathcal{P}_i$, is derived from an artificial neural network and ranges between 0 and 1, peaking near unity for correctly identified particles and near zero for misidentified ones [13]. Using $B^+ \to \bar{\Lambda}p\bar{p}p$ data in the sideband mass regions, defined as $m(\bar{\Lambda}p\bar{p}p) \in [4700, 5049] \cup [5529, 5800]$ MeV$/c^2$, along with simulated B^+ signal decays, the selection criteria are optimized separately for the long and downstream categories to enhance the signal significance $S/\sqrt{S+B}$, even if the signal is somewhat lower than that expected. Here, S and B denote the expected signal and background yields within the signal region $m(\bar{\Lambda}p\bar{p}p) \in [5254, 5304]$ MeV$/c^2$. A common requirement $\log(\chi^2_{\mathrm{IP}}) < 1.8(1.6)$, along with a selection on the variable $\prod_i \mathcal{P}_i > 0.6(0.7)$, is applied to the long (downstream) Λ category for the signal and normalization channels. With respect to preselection criteria,

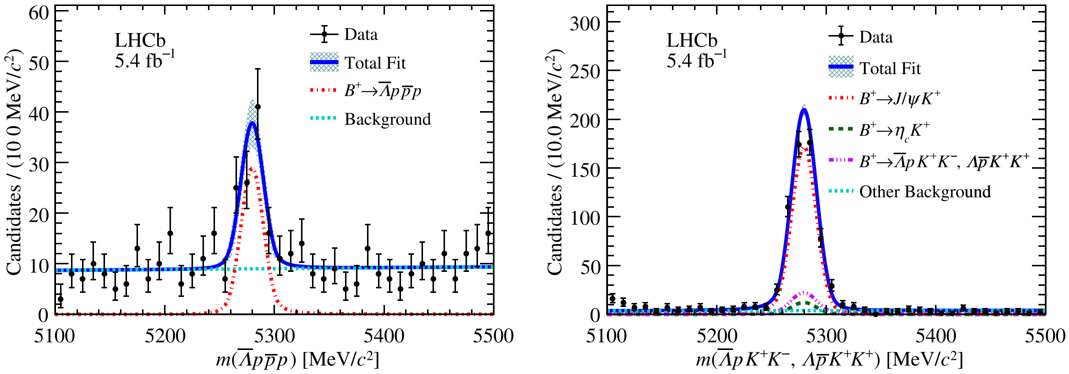

FIG. 1. Invariant-mass distributions of (left) $B^+\to\bar{\Lambda}p\bar{p}p$ with $m(\bar{p}p) < 2850$ MeV/c^2 and (right) $B^+\to J/\psi(\to\bar{\Lambda}pK^-)K^+$ candidates, after combining the long and downstream Λ categories and requiring all selection criteria described in the text. The fit results are shown together with the fit model components. The hashed cyan bands represent the $\pm1\sigma$ model uncertainties from the covariance matrices of the best-fit parameters.

the final selection criteria reduces background by a factor of 5 while retaining about 65% of the signal. To avoid experimenter bias, data in the $B^+\to\bar{\Lambda}p\bar{p}p$ signal region are examined only after all selection criteria are finalized.

Reconstruction efficiencies for signal and normalization channels are evaluated using simulated decays generated uniformly in phase space. To correct the kinematic distributions in the simulated samples, candidates are assigned weights derived from background-subtracted $B^+\to H_{c\bar{c}}(\to\bar{\Lambda}pK^-)K^+$ candidates, where $H_{c\bar{c}}$ represents a J/ψ or η_c meson. Weighting depends on $\chi^2_{\rm IP}$ of the B^+ candidate, track multiplicity in the event, and the momentum of each final-state particle. Additionally, the invariant-mass distributions of the two-body combinations of the final-state particles in simulation are corrected to match the corresponding distributions in data. For the normalization channel, the $m(pK^-)$ versus $m(\bar{\Lambda}K)$ distributions are corrected, while for the signal channel, the $m(\bar{\Lambda}p)$ versus $m(\bar{p}p)$ distributions are corrected to better match the data after the decay is observed.

Several B^+ decays with intermediate charmonium resonances can contribute to the $\bar{\Lambda}p\bar{p}p$ final state, including $B^+\to\bar{\Lambda}pJ/\psi(\to\bar{p}p)$ and $B^+\to\bar{\Lambda}p\eta_c(\to\bar{p}p)$. The $B^+\to\bar{\Lambda}p\bar{p}p$ candidates are divided into three disjoint categories: noncharmonium candidates with $m(\bar{p}p)<2850\,{\rm MeV}/c^2$, $B^+\to\bar{\Lambda}p\eta_c(\to\bar{p}p)$ candidates with $|m(\bar{p}p)-M_{\eta_c}|<40\,{\rm MeV}/c^2$, and $B^+\to\bar{\Lambda}pJ/\psi(\to\bar{p}p)$ candidates with $|m(\bar{p}p)-M_{J/\psi}|<30\,{\rm MeV}/c^2$, where M_{η_c} and $M_{J/\psi}$ are the known η_c and J/ψ masses [27]. The wider window for $B^+\to\bar{\Lambda}p\eta_c(\to\bar{p}p)$ than for $B^+\to\bar{\Lambda}pJ/\psi(\to\bar{p}p)$ accounts for the larger η_c natural linewidth.

The invariant-mass distributions $m(\bar{\Lambda}p\bar{p}p)$ with $m(p\bar{p}) < 2850$ MeV/c^2 and $m(\bar{\Lambda}pKK)$ are shown in Fig. 1. Because of the different available phase space, the final-state particles in the signal decay have lower momenta, resulting in an improved reconstructed mass resolution. Unbinned maximum-likelihood fits are performed to determine the signal yields. The signal shapes are described by a modified Gaussian function with tails on both sides of the peak (double-sided Crystal Ball [28], DSCB) whose values are fixed from simulation. The B^+ mass and width are allowed to vary independently. The background shapes are described by linear functions with coefficients that are free to vary. The B^+ signal yield obtained from the fit to the $m(\bar{\Lambda}p\bar{p}p)$ selected candidates is $N(B^+\to\bar{\Lambda}p\bar{p}p) = 78\pm12$ events, accounting for statistical uncertainties only.

The absolute branching fraction $\mathcal{B}(B^+\to\bar{\Lambda}p\bar{p}p)$ is determined from a simultaneous unbinned maximum-likelihood fit to the signal and the normalization channels. In the normalization channel $B^+\to J/\psi(\to\bar{\Lambda}pK^-+{\rm c.c.})K^+$, decays of $B^+\to\eta_c(\to\bar{\Lambda}pK^-+{\rm c.c.})K^+$, and nonresonant $B^+\to\bar{\Lambda}pK^+K^-$ and $B^+\to\Lambda\bar{p}K^+K^+$ can produce physics backgrounds. To account for these, $B^+\to J/\psi(\to\bar{\Lambda}pK^-+{\rm c.c.})K^+$ candidates are divided into three categories based on the invariant mass $m(\bar{\Lambda}pK^-)$: (i) candidates with $|m(\bar{\Lambda}pK^-)-M_{J/\psi}| < 30$ MeV/c^2 are considered from $B^+\to J/\psi(\to\bar{\Lambda}pK^-)K^+$ decay, (ii) candidates with $|m(\bar{\Lambda}pK^-)-M_{\eta_c}| < 30$ MeV/c^2 are considered from $B^+\to\eta_c(\to\bar{\Lambda}pK^-)K^+$ decay [The $m(\bar{\Lambda}pK^-)$ observed width is approximately 13.8 MeV/c^2 for $\eta_c\to\bar{\Lambda}pK^-$ and 4.2 MeV/c^2 for $J/\psi\to\bar{\Lambda}pK^-$], and (iii) candidates with $3200 < m(\bar{\Lambda}pK^-) < 3300$ MeV/c^2 are considered from charmless $B^+\to\bar{\Lambda}pK^+K^-$ and $B^+\to\Lambda\bar{p}K^+K^+$ decays. For each decay mode, the invariant-mass distributions $m(\bar{\Lambda}pK^+K^-)$ and $m(\Lambda\bar{p}K^+K^+)$ are modeled using DSCB functions. The background yields of $B^+\to\eta_c(\to\bar{\Lambda}pK^-)K^+$, $B^+\to\bar{\Lambda}pK^+K^-$, and $B^+\to\Lambda\bar{p}K^+K^+$ decays in category (i) are extrapolated from the B^+ signal yields in categories (ii) and (iii). Individual contributions within the J/ψ mass window are estimated using extrapolations from simulated data.

The background-subtracted invariant-mass spectra of $\bar{\Lambda}p$ and $\bar{p}p$ pairs, obtained using the *sPlot* technique in the $m(\bar{\Lambda}p\bar{p}p)$ dimension [29], are shown in Fig. 2. The two

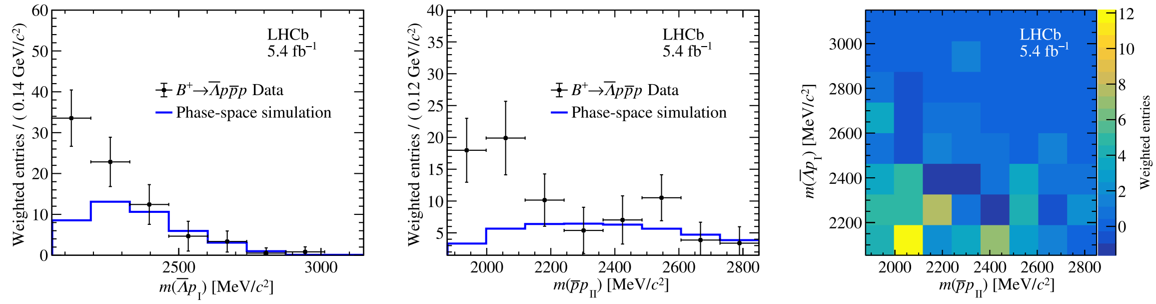

FIG. 2. Distributions of background-subtracted (left) $m(\bar{\Lambda}p_{\rm I})$ and (middle) $m(\bar{p}p_{\rm II})$ for $B^+ \to \bar{\Lambda}p\bar{p}p$ events in data compared with phase-space simulation, where the proton $p_{\rm I}$ yields the lower invariant mass $m(\bar{\Lambda}p)$ with $\bar{\Lambda}$ baryon. Right: two-dimensional distribution of $m(\bar{\Lambda}p_{\rm I})$ and $m(\bar{p}p_{\rm II})$ in data.

identical protons in the final state are distinguished based on the invariant masses formed with the $\bar{\Lambda}$ baryon. The proton that yields the lower invariant mass $m(\bar{\Lambda}p)$ is labeled as $p_{\rm I}$. The other proton, $p_{\rm II}$, is paired with the antiproton to form the second baryon-antibaryon combination. A double threshold enhancement is observed, indicated by the clear accumulation of events in the lower left-hand corner of the weighted $[m(\bar{\Lambda}p_{\rm I}), m(\bar{p}p_{\rm II})]$ distribution, as well as by the peaks near the kinematic thresholds in the $m(\bar{\Lambda}p_{\rm I})$ and $m(\bar{p}p_{\rm II})$ spectra. Similar results, obtained by pairing the proton and antiproton with the lower invariant mass, are shown in the End Matter.

The $m(\bar{\Lambda}p\bar{p}p)$ distribution of candidates with $|m(\bar{p}p) - M_{\eta_c}| < 40\ {\rm MeV}/c^2$ is shown in Fig. 3. The signal shape is modeled by a DSCB function and the background by a threshold function of the form $(x - x_0)^\beta$, where $x_0 \equiv M_\Lambda + M_{\eta_c} + M_p$ and β is a free parameter of the fit. The yield in this region is $N[B^+ \to \bar{\Lambda}p\eta_c(\to \bar{p}p)] = 2.9 \pm 1.9$ events. The yield in the region $|m(\bar{p}p) - M_{J/\psi}| < 30\,{\rm MeV}/c^2$ is $N[B^+ \to \bar{\Lambda}pJ/\psi(\to \bar{p}p)] = 16.4 \pm 4.2$ events. This is consistent with estimates from the known branching fractions $\mathcal{B}(B^+ \to \bar{\Lambda}pJ/\psi)$ and $\mathcal{B}(J/\psi \to p\bar{p})$ [27] and the number of events observed in the normalization channel.

The dominant sources of systematic uncertainty affecting the branching fraction measurements are listed in Table I, and include those associated with the fit models, efficiencies, PID performance, and the branching fraction of the normalization channel.

Three sources of associated systematic uncertainties are estimated from simulation. First are the uncertainties on the nominal efficiencies due to the sizes of the simulated samples. Second are the uncertainties due to the weights used for correcting kinematic differences between simulation and data, assessed by recalculating the branching fractions without applying the weights. The resulting deviation is taken as a conservative estimate of the associated uncertainty. Third are uncertainties on the tracking efficiencies, due to the detector material budget distribution or to the particle interaction cross-sections, that lead to uncertainties on the efficiency ratios. Differences between PID efficiencies in data and simulation are corrected using a combination of simulated and data calibration samples. The signal shapes are varied in two ways: the DSCB function parameters are varied within their uncertainties, and the signal shape is modified to

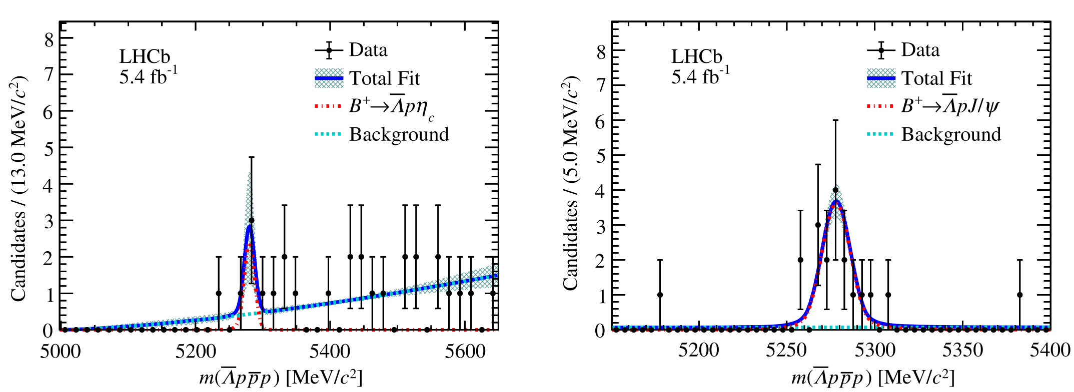

FIG. 3. Invariant-mass distribution of (left) $B^+ \to \bar{\Lambda}p\eta_c(\to \bar{p}p)$ candidates with $|m(\bar{p}p) - M_{\eta_c}| < 40\ {\rm MeV}/c^2$ and (right) $B^+ \to \bar{\Lambda}pJ/\psi(\to \bar{p}p)$ candidates with $|m(\bar{p}p) - M_{J/\psi}| < 30\ {\rm MeV}/c^2$, after combining the long and downstream Λ categories and requiring all selection criteria described in the text. The fit results are shown together with the fit model components. The hashed cyan bands represent the 1σ model uncertainty on the covariance matrix of the best-fit parameters.

TABLE I. Summary of relative systematic uncertainties on (A) $\mathcal{B}(B^+ \to \bar{\Lambda} p \bar{p} p)$ and (B) $\mathcal{B}(B^+ \to \bar{\Lambda} p \eta_c(\to \bar{p} p))$, in percent. The total systematic uncertainty is computed as the square root of the sum of squared sum in quadrature of individual contributions. There is no model correction for $B^+ \to \bar{\Lambda} p \eta_c(\to \bar{p} p)$ decay due to the small size of this component. The last row indicates the relative statistical uncertainty.

Systematic source	A	B
Simulated sample size	0.6	0.6
Kinematic correction	1.4	1.4
Tracking	1.2	1.2
PID	3.1	2.0
Signal shape	2.9	31.1
Background shape	1.2	2.4
Model correction (signal)	2.7	...
Model correction (normalization)	1.6	1.6
Nonresonant	...	22.9
Total systematic	5.8	38.8
Statistical uncertainty	16.4	65.5

include a Gaussian function together with the DSCB function. For the $B^+ \to \bar{\Lambda} p \bar{p} p$ decay, the background model is replaced by a second-order polynomial function. For the $B^+ \to \bar{\Lambda} p \eta_c(\to \bar{p} p)$ decay, the threshold background shape is replaced by an exponential function. Concerning the correction of decay models for signal and normalization channels in simulation, the parameters that affect the performance of the weighting algorithm are varied individually, and the total efficiencies are recalculated using the alternative sets of weights, with the largest deviation taken as a systematic uncertainty. For $B^+ \to \bar{\Lambda} p \bar{p} p$ decay, an alternative correction based on the decay model shown in Fig. 4 is implemented and the resulting deviation is taken as an additional contribution to the systematic uncertainty associated with the signal model correction. For the $B^+ \to \bar{\Lambda} p \eta_c(\to \bar{p} p)$ decay, the dominant systematic uncertainties relate to the signal shape and the potential contribution from charmless $B^+ \to \bar{\Lambda} p \bar{p} p$ decay, which is estimated by extrapolating the observed yield with $m(\bar{p} p) < 2850\ \mathrm{MeV}/c^2$ into the η_c mass window.

The CP asymmetry of the $B^+ \to \bar{\Lambda} p \bar{p} p$ decay rate integrated over the phase space is measured by fitting the B^+ and B^- samples separately, as shown in the End Matter, using the same procedure as for the branching fraction measurement. The yields vary independently, while the shape parameters are shared between the B^+ and B^- candidates. The raw asymmetry (A_{raw}) between the B^+ and B^- signal yields is found to be $(5.6 \pm 15.5)\%$. To obtain the CP asymmetry, this must be corrected as per

$$\mathcal{A}_{CP} = A_{\mathrm{raw}} - A_{\mathrm{prod}} - A_{\mathrm{det}},$$

where A_{prod} is the production asymmetry of $B^{\pm}$ mesons and A_{det} is the sum of the instrumental asymmetries in detection (A_{D}), PID (A_{PID}), and trigger (A_{trigger}) of particles and antiparticles.

The production asymmetry has been measured by LHCb to be $(-0.7 \pm 0.3)\%$ [30]. The trigger asymmetry arises from differences in trigger efficiencies between charge-conjugated final states. The efficiency for a charged hadron to be responsible for the affirmative decision of the hardware trigger is determined as a function of p_{T}, separately for positively and negatively charged particles [17]. The asymmetry introduced by the hardware trigger for candidates is determined to be $A_{\mathrm{trigger}}^{\bar{\Lambda} p \bar{p} p} = (0.03 \pm 0.18)\%$. The proton detection asymmetry is evaluated as a function of momentum using the method developed in Ref. [31], and is measured to be $A_{\mathrm{D}}^{p \bar{p} p} = (1.15 \pm 0.66)\%$. The detection asymmetry for the Λ baryon is estimated by parametrizing the detection asymmetries of the proton and pion as functions of their momentum and, in the case of the pion, also pseudorapidity [31,32], and is measured to be $A_{\mathrm{D}}^{\bar{\Lambda}} = (-1.49 \pm 0.26)\%$. The PID asymmetry is evaluated using calibration samples that account for differences in PID efficiency between positively and negatively charged tracks and is determined to be $A_{\mathrm{PID}}^{p \bar{p} p} = (0.18 \pm 1.50)\%$.

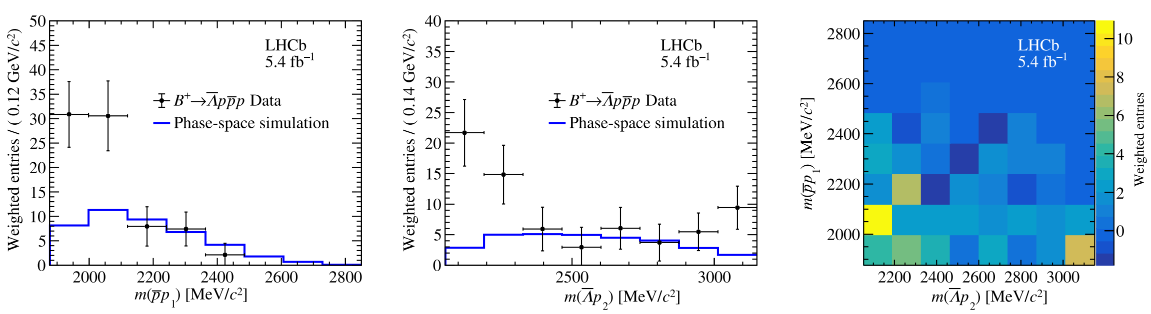

FIG. 4. Distributions of background-subtracted (left) $m(\bar{p} p_1)$ and (middle) $m(\bar{\Lambda} p_2)$ for $B^+ \to \bar{\Lambda} p \bar{p} p$ events in data compared with phase-space simulation, where the proton p_1 yields the lower invariant mass with antiproton. Right: two-dimensional distribution of $m(\bar{p} p_1)$ and $m(\bar{\Lambda} p_2)$ in data.

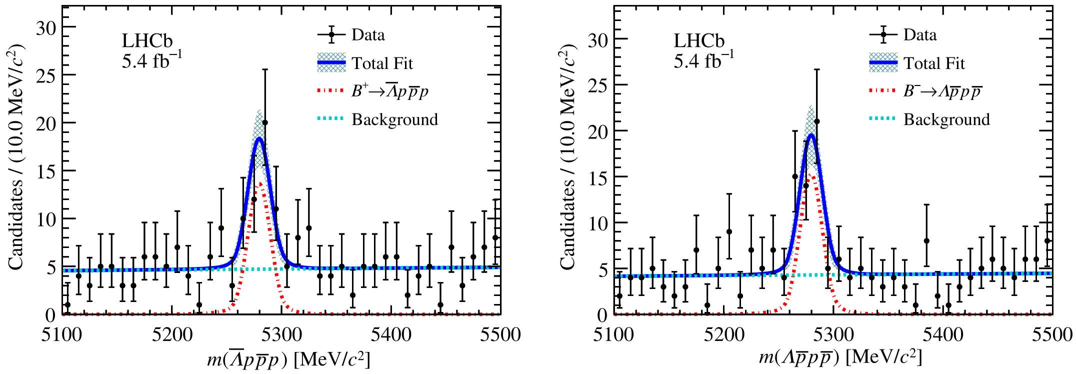

FIG. 5. Invariant-mass distribution of (left) $B^+ \to \bar{\Lambda} p \bar{p} p$ and (right) $B^- \to \Lambda \bar{p} p \bar{p}$ candidates, after combining the long and downstream Λ categories and requiring all selection criteria described in the text. The fit results for these samples are shown together with the fit model components. The hashed cyan bands represent the 1σ model uncertainty on the covariance matrix of the best-fit parameters.

The PID asymmetry from the Λ baryon is negligible due to its loose selection criteria.

The estimation of model-related systematic uncertainties in the determination of $A_{\rm raw}$ is performed using the same procedure as for the branching fraction measurement. The differences between the raw asymmetries determined by the two sets of fits are added in quadrature, and the resulting value is taken as a systematic uncertainty. Altogether with the uncertainties on external asymmetries, the CP asymmetry is measured to be $\mathcal{A}_{CP} = (5.4 \pm 15.6 \pm 2.4)\%$.

In summary, a new charmless and purely baryonic decay mode of the B^+ meson, $B^+ \to \bar{\Lambda} p \bar{p} p$, is observed. The signal yield is measured to be $N(B^+ \to \bar{\Lambda} p \bar{p} p) = 78 \pm 12$ events. The branching fraction relative to the normalization channel is determined to be $\mathcal{B}(B^+ \to \bar{\Lambda} p \bar{p} p)/\mathcal{B}(B^+ \to J/\psi(\to \bar{\Lambda} p K^-)K^+) = (0.245 \pm 0.040 \pm 0.014)$, where the uncertainties are statistical and systematic, respectively. The branching fraction is measured to be

$$\mathcal{B}(B^+ \to \bar{\Lambda} p \bar{p} p) = (2.15 \pm 0.35 \pm 0.12 \pm 0.28) \times 10^{-7},$$

where the first uncertainty is statistical, the second systematic, and the third arises from the external branching fraction of the normalization channel. This result is lower than, but in reasonable agreement with, a SM prediction of $\mathcal{B}(B^+ \to \bar{\Lambda} p \bar{p} p) = (7.4^{+0.6}_{-0.2} \pm 0.03^{+3.6}_{-2.6}) \times 10^{-7}$ [7], where the uncertainty arises from nonfactorizable QCD corrections, the CKM matrix-element inputs, and form-factor modeling. The CP asymmetry is measured to be $\mathcal{A}_{CP} = (5.4 \pm 15.6 \pm 2.4)\%$, with the first uncertainty statistical and the second systematic. The background-subtracted mass spectra exhibit a clear double-threshold enhancement in both baryon-antibaryon invariant-mass distributions close to their thresholds, which plays an enhancing factor [7] in the $B^+ \to \bar{\Lambda} p \bar{p} p$ decay and may reveal resonant structures such as the $X(1835)$ baryonium bound state [9].

In the region defined by $|m(\bar{p}p) - M_{\eta_c}| < 40$ MeV$/c^2$, the yield of $B^+ \to \bar{\Lambda} p \eta_c(\to \bar{p}p)$ is $N[B^+ \to \bar{\Lambda} p \eta_c(\to \bar{p}p)] = 2.9 \pm 1.9$ events. The corresponding branching fraction is

$$\mathcal{B}(B^+ \to \bar{\Lambda} p \eta_c(\to \bar{p}p)) = (8.3 \pm 5.4 \pm 3.2 \pm 1.1) \times 10^{-9},$$

where the first uncertainty is statistical, the second systematic, and the third arises from the external branching fraction of the normalization channel. The 90% confidence level upper limit on the branching fraction is $\mathcal{B}(B^+ \to \bar{\Lambda} p \eta_c(\to \bar{p}p)) < 2.1 \times 10^{-8}$.

The measurement of $\mathcal{B}(B^+ \to \bar{\Lambda} p \bar{p} p)$ constrains models of perturbative QCD effects in multibody baryonic final states, particularly in regions where large theoretical uncertainties remain [7]. The threshold enhancements manifested in this Letter highlight the rich dynamics of baryonic B decays and should stimulate further theoretical studies.

Acknowledgments—We express our gratitude to our colleagues in the CERN accelerator departments for the excellent performance of the LHC. We thank the technical and administrative staff at the LHCb institutes. We acknowledge support from CERN and from the national agencies: ARC (Australia); CAPES, CNPq, FAPERJ, and FINEP (Brazil); MOST and NSFC (China); CNRS/IN2P3 (France); BMBF, DFG, and MPG (Germany); INFN (Italy); NWO (Netherlands); MNiSW and NCN (Poland); MCID/IFA (Romania); MICIU and AEI (Spain); SNSF and SER (Switzerland); NASU (Ukraine); STFC (United Kingdom); DOE NP and NSF (USA). We acknowledge the computing resources that are provided by ARDC (Australia), CBPF (Brazil), CERN, IHEP and LZU (China), IN2P3 (France), KIT and DESY (Germany), INFN (Italy), SURF (Netherlands), Polish WLCG (Poland), IFIN-HH (Romania), PIC (Spain), CSCS (Switzerland), and

GridPP (United Kingdom). We are indebted to the communities behind the multiple open-source software packages on which we depend. Individual groups or members have received support from Key Research Program of Frontier Sciences of CAS, CAS PIFI, CAS CCEPP, Fundamental Research Funds for the Central Universities, and Sci. & Tech. Program of Guangzhou (China); Minciencias (Colombia); EPLANET, Marie Skłodowska-Curie Actions, ERC, and NextGenerationEU (European Union); A*MIDEX, ANR, IPhU and Labex P2IO, and Région Auvergne-Rhône-Alpes (France); Alexander-von-Humboldt Foundation (Germany); ICSC (Italy); Severo Ochoa and María de Maeztu Units of Excellence, GVA, XuntaGal, GENCAT, InTalent-Inditex, and Prog. Atracción Talento CM (Spain); SRC (Sweden); the Leverhulme Trust, the Royal Society and UKRI (United Kingdom).

Data availability—The data that support the findings of this article are openly available [33].

[1] H. Albrecht *et al.* (ARGUS Collaboration), Observation of the charmless B meson decays, Phys. Lett. B **209**, 119 (1988).
[2] K. Abe *et al.* (Belle Collaboration), Observation of $B^\pm \to p\bar{p}K^\pm$, Phys. Rev. Lett. **88**, 181803 (2002).
[3] M.-Z. Wang *et al.* (Belle Collaboration), Observation of $B^+ \to p\bar{p}\pi^+$, $B^0 \to p\bar{p}K^0$, and $B^+ \to p\bar{p}K^{*+}$, Phys. Rev. Lett. **92**, 131801 (2004).
[4] R. Aaij *et al.* (LHCb Collaboration), Observation of charmless baryonic decays $B^0_{(s)} \to p\bar{p}h^+h'^-$, Phys. Rev. D **96**, 051103 (2017).
[5] H.-Y. Cheng and K.-C. Yang, Charmless exclusive baryonic B decays, Phys. Rev. D **66**, 014020 (2002).
[6] C.-K. Chua, W.-S. Hou, and S.-Y. Tsai, Charmless three-body baryonic B decays, Phys. Rev. D **66**, 054004 (2002).
[7] Y.-K. Hsiao, Four-body baryonic $B \to B_1\bar{B}'_1B_2\bar{B}'_2$ decays, Phys. Lett. B **845**, 138158 (2023).
[8] R. Aaij *et al.* (LHCb Collaboration), Measurement of the branching fractions $B^0 \to p\bar{p}p\bar{p}$ and $B^0_s \to p\bar{p}p\bar{p}$, Phys. Rev. Lett. **131**, 091901 (2023).
[9] M. Ablikim *et al.* (BESIII Collaboration), Spin-parity analysis of $p\bar{p}$ mass threshold structure in J/ψ and $\psi(3686)$ radiative decays, Phys. Rev. Lett. **108**, 112003 (2012).
[10] M. Ablikim *et al.* (BESIII Collaboration), Determination of spin-parity quantum numbers for the narrow structure near the $p\bar{\Lambda}$ threshold in $e^+e^- \to pK^-\bar{\Lambda}$ + c.c., Phys. Rev. Lett. **131**, 151901 (2023).
[11] C. Q. Geng, Y. K. Hsiao, and J. N. Ng, Direct *CP* violation in $B^\pm \to p\bar{p}K^{(*)\pm}$, Phys. Rev. Lett. **98**, 011801 (2007).
[12] A. A. Alves Jr. *et al.* (LHCb Collaboration), The LHCb detector at the LHC, J. Instrum. **3**, S08005 (2008).
[13] LHCb Collaboration, LHCb detector performance, Int. J. Mod. Phys. A **30**, 1530022 (2015).
[14] R. Aaij *et al.*, Performance of the LHCb vertex locator, J. Instrum. **9**, P09007 (2014).
[15] P. d'Argent *et al.*, Improved performance of the LHCb outer tracker in LHC Run 2, J. Instrum. **12**, P11016 (2017).
[16] M. Adinolfi *et al.*, Performance of the LHCb RICH detector at the LHC, Eur. Phys. J. C **73**, 2431 (2013).
[17] R. Aaij *et al.*, The LHCb trigger and its performance in 2011, J. Instrum. **8**, P04022 (2013).
[18] T. Likhomanenko, P. Ilten, E. Khairullin, A. Rogozhnikov, A. Ustyuzhanin, and M. Williams, LHCb topological trigger reoptimization, J. Phys. Conf. Ser. **664**, 082025 (2015).
[19] T. Sjöstrand, S. Mrenna, and P. Skands, A brief introduction to PYTHIA 8.1, Comput. Phys. Commun. **178**, 852 (2008).
[20] I. Belyaev *et al.*, Handling of the generation of primary events in Gauss, the LHCb simulation framework, J. Phys. Conf. Ser. **331**, 032047 (2011).
[21] D. J. Lange, The EvtGen particle decay simulation package, Nucl. Instrum. Methods Phys. Res., Sect. A **462**, 152 (2001).
[22] N. Davidson, T. Przedzinski, and Z. Was, PHOTOS interface in C++: Technical and physics documentation, Comput. Phys. Commun. **199**, 86 (2016).
[23] S. Agostinelli *et al.* (Geant4 Collaboration), Geant4: A simulation toolkit, Nucl. Instrum. Methods Phys. Res., Sect. A **506**, 250 (2003).
[24] J. Allison *et al.* (Geant4 Collaboration), Geant4 developments and applications, IEEE Trans. Nucl. Sci. **53**, 270 (2006).
[25] M. Clemencic, G. Corti, S. Easo, C. R. Jones, S. Miglioranzi, M. Pappagallo, and P. Robbe, The LHCb simulation application, Gauss: Design, evolution and experience, J. Phys. Conf. Ser. **331**, 032023 (2011).
[26] M. De Cian, S. Farry, P. Seyfert, and S. Stahl, Fast neural-net based fake track rejection in the LHCb reconstruction, Report No. LHCb-PUB-2017-011, CERN, 2017.
[27] S. Navas *et al.* (Particle Data Group), Review of particle physics, Phys. Rev. D **110**, 030001 (2024).
[28] T. Skwarnicki, A study of the radiative cascade transitions between the Upsilon-prime and Upsilon resonances, PhD thesis, Institute of Nuclear Physics, Krakow, 1986; DESY-F31-86-02.
[29] M. Pivk and F. R. Le Diberder, sPlot: A statistical tool to unfold data distributions, Nucl. Instrum. Methods Phys. Res., Sect. A **555**, 356 (2005).
[30] R. Aaij *et al.* (LHCb Collaboration), Direct *CP* violation in charmless three-body decays of $B^\pm$ mesons, Phys. Rev. D **108**, 012008 (2023).
[31] R. Aaij *et al.* (LHCb Collaboration), Observation of a $\Lambda^0_b - \bar{\Lambda}^0_b$ production asymmetry in proton-proton collisions at $\sqrt{s} = 7$ and 8 TeV, J. High Energy Phys. 10 (2021) 060.
[32] R. Aaij *et al.* (LHCb Collaboration), Observation of the mass difference between neutral charm-meson eigenstates, Phys. Rev. Lett. **127**, 111801 (2021); Phys. Rev. Lett. **131**, 079901(E) (2023).
[33] https://cds.cern.ch/record/2940817.

End Matter

Additional baryon-antibaryon mass spectra—Another study of baryon-antibaryon invariant-mass spectra in the $B^+ \to \bar{\Lambda} p \bar{p} p$ decay is shown in Fig. 4. The two identical protons in the final state are distinguished based on the invariant mass formed with the antiproton rather than with the $\bar{\Lambda}$ baryon. The $\bar{p} p$ combination that yields the lower invariant mass is labeled as $\bar{p} p_1$. The remaining proton, p_2, is then paired with the $\bar{\Lambda}$ baryon to form the second baryon-antibaryon combination.

As expected due to the definition of the pairs, the enhancement here is greater for $m(\bar{p} p)$ than in Fig. 2 and less for $m(\bar{\Lambda} p)$. Qualitatively, however, the conclusion is the same and enhancements are observed in the lower left-hand corner of the scatter plot and in both projections.

Fit to different charged B samples—Figure 5 shows the fits to the $B^+ \to \bar{\Lambda} p \bar{p} p$ and $B^- \to \Lambda \bar{p} p \bar{p}$ samples for the measurement of $\mathcal{A}_{CP}$.

R. Aaij,[38] A. S. W. Abdelmotteleb,[57] C. Abellan Beteta,[51] F. Abudinén,[57] T. Ackernley,[61] A. A. Adefisoye,[69] B. Adeva,[47] M. Adinolfi,[55] P. Adlarson,[85] C. Agapopoulou,[14] C. A. Aidala,[87] Z. Ajaltouni,[11] S. Akar,[11] K. Akiba,[38] P. Albicocco,[28] J. Albrecht,[19,b] R. Aleksiejunas,[80] F. Alessio,[49] P. Alvarez Cartelle,[56] R. Amalric,[16] S. Amato,[3] J. L. Amey,[55] Y. Amhis,[14] L. An,[6] L. Anderlini,[27] M. Andersson,[51] P. Andreola,[51] M. Andreotti,[26] S. Andres Estrada,[84] A. Anelli,[31,49,c] D. Ao,[7] C. Arata,[12] F. Archilli,[37,d] Z Areg,[69] M. Argenton,[26] S. Arguedas Cuendis,[9,49] L. Arnone,[31,c] A. Artamonov,[44] M. Artuso,[69] E. Aslanides,[13] R. Ataíde Da Silva,[50] M. Atzeni,[65] B. Audurier,[12] J. A. Authier,[15] D. Bacher,[64] I. Bachiller Perea,[50] S. Bachmann,[22] M. Bachmayer,[50] J. J. Back,[57] P. Baladron Rodriguez,[47] V. Balagura,[15] A. Balboni,[26] W. Baldini,[26] Z. Baldwin,[78] L. Balzani,[19] H. Bao,[7] J. Baptista de Souza Leite,[2] C. Barbero Pretel,[47,12] M. Barbetti,[27] I. R. Barbosa,[70] R. J. Barlow,[63] M. Barnyakov,[25] S. Barsuk,[14] W. Barter,[59] J. Bartz,[69] S. Bashir,[40] B. Batsukh,[5] P. B. Battista,[14] A. Bay,[50] A. Beck,[65] M. Becker,[19] F. Bedeschi,[35] I. B. Bediaga,[2] N. A. Behling,[19] S. Belin,[47] A. Bellavista,[25] K. Belous,[44] I. Belov,[29] I. Belyaev,[36] G. Benane,[13] G. Bencivenni,[28] E. Ben-Haim,[16] A. Berezhnoy,[44] R. Bernet,[51] S. Bernet Andres,[46] A. Bertolin,[33] C. Betancourt,[51] F. Betti,[59] J. Bex,[56] Ia. Bezshyiko,[51] O. Bezshyyko,[86] J. Bhom,[41] M. S. Bieker,[18] N. V. Biesuz,[26] P. Billoir,[16] A. Biolchini,[38] M. Birch,[62] F. C. R. Bishop,[10] A. Bitadze,[63] A. Bizzeti,[27,e] T. Blake,[57,f] F. Blanc,[50] J. E. Blank,[19] S. Blusk,[69] V. Bocharnikov,[44] J. A. Boelhauve,[19] O. Boente Garcia,[15] T. Boettcher,[68] A. Bohare,[59] A. Boldyrev,[44] C. S. Bolognani,[82] R. Bolzonella,[26,g] R. B. Bonacci,[1] N. Bondar,[44,49] A. Bordelius,[49] F. Borgato,[33,49] S. Borghi,[63] M. Borsato,[31,c] J. T. Borsuk,[83] E. Bottalico,[61] S. A. Bouchiba,[50] M. Bovill,[64] T. J. V. Bowcock,[61] A. Boyer,[49] C. Bozzi,[26] J. D. Brandenburg,[88] A. Brea Rodriguez,[50] N. Breer,[19] J. Brodzicka,[41] A. Brossa Gonzalo,[47,a] J. Brown,[61] D. Brundu,[32] E. Buchanan,[59] M. Burgos Marcos,[82] A. T. Burke,[63] C. Burr,[49] C. Buti,[27] J. S. Butter,[56] J. Buytaert,[49] W. Byczynski,[49] S. Cadeddu,[32] H. Cai,[75] Y. Cai,[5] A. Caillet,[16] R. Calabrese,[26,g] S. Calderon Ramirez,[9] L. Calefice,[45] M. Calvi,[31,c] M. Calvo Gomez,[46] P. Camargo Magalhaes,[2,h] J. I. Cambon Bouzas,[47] P. Campana,[28] D. H. Campora Perez,[82] A. F. Campoverde Quezada,[7] S. Capelli,[31] M. Caporale,[25] L. Capriotti,[26] R. Caravaca-Mora,[9] A. Carbone,[25,i] L. Carcedo Salgado,[47] R. Cardinale,[29,j] A. Cardini,[32] P. Carniti,[31] L. Carus,[22] A. Casais Vidal,[65] R. Caspary,[22] G. Casse,[61] M. Cattaneo,[49] G. Cavallero,[26] V. Cavallini,[26,g] S. Celani,[22] I. Celestino,[35,k] S. Cesare,[30,l] F. Cesario Laterza Lopes,[2] A. J. Chadwick,[61] I. Chahrour,[87] H. Chang,[4,m] M. Charles,[16] Ph. Charpentier,[49] E. Chatzianagnostou,[38] R. Cheaib,[79] M. Chefdeville,[10] C. Chen,[56] J. Chen,[50] S. Chen,[5] Z. Chen,[7] M. Cherif,[12] A. Chernov,[41] S. Chernyshenko,[53] X. Chiotopoulos,[82] V. Chobanova,[84] M. Chrzaszcz,[41] A. Chubykin,[44] V. Chulikov,[28,36,49] P. Ciambrone,[28] X. Cid Vidal,[47] G. Ciezarek,[49] P. Cifra,[38] P. E. L. Clarke,[59] M. Clemencic,[49] H. V. Cliff,[56] J. Closier,[49] C. Cocha Toapaxi,[22] V. Coco,[49] J. Cogan,[13] E. Cogneras,[11] L. Cojocariu,[43] S. Collaviti,[50] P. Collins,[49] T. Colombo,[49] M. Colonna,[19] A. Comerma-Montells,[45] L. Congedo,[24] J. Connaughton,[57] A. Contu,[32] N. Cooke,[60] G. Cordova,[35,k] C. Coronel,[66] I. Corredoira,[12] A. Correia,[16] G. Corti,[49] J. Cottee Meldrum,[55] B. Couturier,[49] D. C. Craik,[51] M. Cruz Torres,[2,n] E. Curras Rivera,[50] R. Currie,[59] C. L. Da Silva,[68] S. Dadabaev,[44] L. Dai,[72] X. Dai,[4] E. Dall'Occo,[49] J. Dalseno,[84]

C. D'Ambrosio,[62] J. Daniel,[11] P. d'Argent,[24] G. Darze,[3] A. Davidson,[57] J. E. Davies,[63]
O. De Aguiar Francisco,[63] C. De Angelis,[32,o] F. De Benedetti,[49] J. de Boer,[38] K. De Bruyn,[81] S. De Capua,[63]
M. De Cian,[63] U. De Freitas Carneiro Da Graca,[2,p] E. De Lucia,[28] J. M. De Miranda,[2] L. De Paula,[3]
M. De Serio,[24,q] P. De Simone,[28] F. De Vellis,[19] J. A. de Vries,[82] F. Debernardis,[24] D. Decamp,[10] S. Dekkers,[1]
L. Del Buono,[16] B. Delaney,[65] H.-P. Dembinski,[19] J. Deng,[8] V. Denysenko,[51] O. Deschamps,[11] F. Dettori,[32,o]
B. Dey,[79] P. Di Nezza,[28] I. Diachkov,[44] S. Didenko,[44] S. Ding,[69] Y. Ding,[50] L. Dittmann,[22] V. Dobishuk,[53]
A. D. Docheva,[60] A. Doheny,[57] C. Dong,[4,m] A. M. Donohoe,[23] F. Dordei,[32] A. C. dos Reis,[2] A. D. Dowling,[69]
L. Dreyfus,[13] W. Duan,[73] P. Duda,[83] L. Dufour,[49] V. Duk,[34] P. Durante,[49] M. M. Duras,[83] J. M. Durham,[68]
O. D. Durmus,[79] A. Dziurda,[41] A. Dzyuba,[44] S. Easo,[58] E. Eckstein,[18] U. Egede,[1] A. Egorychev,[44]
V. Egorychev,[44] S. Eisenhardt,[59] E. Ejopu,[61] L. Eklund,[85] M. Elashri,[66] J. Ellbracht,[19] S. Ely,[62] A. Ene,[43]
J. Eschle,[69] S. Esen,[22] T. Evans,[38] F. Fabiano,[32] S. Faghih,[66] L. N. Falcao,[2] B. Fang,[7] R. Fantechi,[35]
L. Fantini,[34,r] M. Faria,[50] K. Farmer,[59] D. Fazzini,[31,c] L. Felkowski,[83] M. Feng,[5,7] M. Feo,[19]
A. Fernandez Casani,[48] M. Fernandez Gomez,[47] A. D. Fernez,[67] F. Ferrari,[25,i] F. Ferreira Rodrigues,[3]
M. Ferrillo,[51] M. Ferro-Luzzi,[49] S. Filippov,[44] R. A. Fini,[24] M. Fiorini,[26,g] M. Firlej,[40] K. L. Fischer,[64]
D. S. Fitzgerald,[87] C. Fitzpatrick,[63] T. Fiutowski,[40] F. Fleuret,[15] A. Fomin,[52] M. Fontana,[25] L. F. Foreman,[63]
R. Forty,[49] D. Foulds-Holt,[59] V. Franco Lima,[3] M. Franco Sevilla,[67] M. Frank,[49] E. Franzoso,[26,g] G. Frau,[63]
C. Frei,[49] D. A. Friday,[63,49] J. Fu,[7] Q. Führing,[19,56,b] T. Fulghesu,[13] G. Galati,[24] M. D. Galati,[38]
A. Gallas Torreira,[47] D. Galli,[25,i] S. Gambetta,[59] M. Gandelman,[3] P. Gandini,[30] B. Ganie,[63] H. Gao,[7] R. Gao,[64]
T. Q. Gao,[56] Y. Gao,[8] Y. Gao,[6] Y. Gao,[8] L. M. Garcia Martin,[50] P. Garcia Moreno,[45] J. García Pardiñas,[65]
P. Gardner,[67] K. G. Garg,[8] L. Garrido,[45] C. Gaspar,[49] A. Gavrikov,[33] L. L. Gerken,[19] E. Gersabeck,[20]
M. Gersabeck,[20] T. Gershon,[57] S. Ghizzo,[29,j] Z. Ghorbanimoghaddam,[55] F. I. Giasemis,[16,s] V. Gibson,[56]
H. K. Giemza,[42] A. L. Gilman,[66] M. Giovannetti,[28] A. Gioventù,[45] L. Girardey,[63,58] M. A. Giza,[41]
F. C. Glaser,[14,22] V. V. Gligorov,[16] C. Göbel,[70] L. Golinka-Bezshyyko,[86] E. Golobardes,[46] D. Golubkov,[44]
A. Golutvin,[62,49] S. Gomez Fernandez,[45] W. Gomulka,[40] I. Gonçales Vaz,[49] F. Goncalves Abrantes,[64]
M. Goncerz,[41] G. Gong,[4,m] J. A. Gooding,[19] I. V. Gorelov,[44] C. Gotti,[31] E. Govorkova,[65] J. P. Grabowski,[30]
L. A. Granado Cardoso,[49] E. Graugés,[45] E. Graverini,[50,t] L. Grazette,[57] G. Graziani,[27] A. T. Grecu,[43]
N. A. Grieser,[66] L. Grillo,[60] S. Gromov,[44] C. Gu,[15] M. Guarise,[26] L. Guerry,[11] V. Guliaeva,[44] P. A. Günther,[22]
A.-K. Guseinov,[50] E. Gushchin,[44] Y. Guz,[6,49] T. Gys,[49] K. Habermann,[18] T. Hadavizadeh,[1] C. Hadjivasiliou,[67]
G. Haefeli,[50] C. Haen,[49] S. Haken,[56] G. Hallett,[57] P. M. Hamilton,[67] J. Hammerich,[61] Q. Han,[33] X. Han,[22,49]
S. Hansmann-Menzemer,[22] L. Hao,[7] N. Harnew,[64] T. H. Harris,[1] M. Hartmann,[14] S. Hashmi,[40] J. He,[7,u]
A. Hedes,[63] F. Hemmer,[49] C. Henderson,[66] R. Henderson,[14] R. D. L. Henderson,[1] A. M. Hennequin,[49]
K. Hennessy,[61] L. Henry,[50] J. Herd,[62] P. Herrero Gascon,[22] J. Heuel,[17] A. Heyn,[13] A. Hicheur,[3]
G. Hijano Mendizabal,[51] J. Horswill,[63] R. Hou,[8] Y. Hou,[11] D. C. Houston,[60] N. Howarth,[61] J. Hu,[73] W. Hu,[7]
X. Hu,[4,m] W. Hulsbergen,[38] R. J. Hunter,[57] M. Hushchyn,[44] D. Hutchcroft,[61] M. Idzik,[40] D. Ilin,[44] P. Ilten,[66]
A. Iniukhin,[44] A. Iohner,[10] A. Ishteev,[44] K. Ivshin,[44] H. Jage,[17] S. J. Jaimes Elles,[77,48,49] S. Jakobsen,[49]
E. Jans,[38] B. K. Jashal,[48] A. Jawahery,[67] C. Jayaweera,[54] V. Jevtic,[19] Z. Jia,[16] E. Jiang,[67] X. Jiang,[5,7]
Y. Jiang,[7] Y. J. Jiang,[6] E. Jimenez Moya,[9] N. Jindal,[88] M. John,[64] A. John Rubesh Rajan,[23] D. Johnson,[54]
C. R. Jones,[56] S. Joshi,[42] B. Jost,[49] J. Juan Castella,[56] N. Jurik,[49] I. Juszczak,[41] D. Kaminaris,[50] S. Kandybei,[52]
M. Kane,[59] Y. Kang,[4,m] C. Kar,[11] M. Karacson,[49] A. Kauniskangas,[50] J. W. Kautz,[66] M. K. Kazanecki,[41]
F. Keizer,[49] M. Kenzie,[56] T. Ketel,[38] B. Khanji,[69] A. Kharisova,[44] S. Kholodenko,[62,49] G. Khreich,[14] T. Kirn,[17]
V. S. Kirsebom,[31,c] O. Kitouni,[65] S. Klaver,[39] N. Kleijne,[35,k] D. K. Klekots,[86] K. Klimaszewski,[42]
M. R. Kmiec,[42] T. Knospe,[19] R. Kolb,[22] S. Koliiev,[53] L. Kolk,[19] A. Konoplyannikov,[6] P. Kopciewicz,[49]
P. Koppenburg,[38] A. Korchin,[52] M. Korolev,[44] I. Kostiuk,[38] O. Kot,[53] S. Kotriakhova, E. Kowalczyk,[67]
A. Kozachuk,[44] P. Kravchenko,[44] L. Kravchuk,[44] O. Kravcov,[80] M. Kreps,[57] P. Krokovny,[44] W. Krupa,[69]
W. Krzemien,[42] O. Kshyvanskyi,[53] S. Kubis,[83] M. Kucharczyk,[41] V. Kudryavtsev,[44] E. Kulikova,[44] A. Kupsc,[85]
V. Kushnir,[52] B. Kutsenko,[13] J. Kvapil,[68] I. Kyryllin,[52] D. Lacarrere,[49] P. Laguarta Gonzalez,[45] A. Lai,[32]
A. Lampis,[32] D. Lancierini,[62] C. Landesa Gomez,[47] J. J. Lane,[1] G. Lanfranchi,[28] C. Langenbruch,[22] J. Langer,[19]
O. Lantwin,[44] T. Latham,[57] F. Lazzari,[35,49,t] C. Lazzeroni,[54] R. Le Gac,[13] H. Lee,[61] R. Lefèvre,[11] A. Leflat,[44]
S. Legotin,[44] M. Lehuraux,[57] E. Lemos Cid,[49] O. Leroy,[13] T. Lesiak,[41] E. D. Lesser,[49] B. Leverington,[22]

A. Li,[4,m] C. Li,[4,m] C. Li,[13] H. Li,[73] J. Li,[8] K. Li,[76] L. Li,[63] M. Li,[8] P. Li,[7] P.-R. Li,[74] Q. Li,[5,7] T. Li,[72] T. Li,[73] Y. Li,[8] Y. Li,[5] Y. Li,[4] Z. Lian,[4,m] Q. Liang,[8] X. Liang,[69] Z. Liang,[32] S. Libralon,[48] A. L. Lightbody,[12] C. Lin,[7] T. Lin,[58] R. Lindner,[49] H. Linton,[62] R. Litvinov,[32] D. Liu,[8] F. L. Liu,[1] G. Liu,[73] K. Liu,[74] S. Liu,[5,7] W. Liu,[8] Y. Liu,[59] Y. Liu,[74] Y. L. Liu,[62] G. Loachamin Ordonez,[70] A. Lobo Salvia,[45] A. Loi,[32] T. Long,[56] J. H. Lopes,[3] A. Lopez Huertas,[45] C. Lopez Iribarnegaray,[47] S. López Soliño,[47] Q. Lu,[15] C. Lucarelli,[49] D. Lucchesi,[33,v] M. Lucio Martinez,[48] Y. Luo,[6] A. Lupato,[33,w] E. Luppi,[26,g] K. Lynch,[23] X.-R. Lyu,[7] G. M. Ma,[4,m] H. Ma,[72] S. Maccolini,[19] F. Machefert,[14] F. Maciuc,[43] B. Mack,[69] I. Mackay,[64] L. M. Mackey,[69] L. R. Madhan Mohan,[56] M. J. Madurai,[54] D. Magdalinski,[38] D. Maisuzenko,[44] J. J. Malczewski,[41] S. Malde,[64] L. Malentacca,[49] A. Malinin,[44] T. Maltsev,[44] G. Manca,[32,o] G. Mancinelli,[13] C. Mancuso,[14] R. Manera Escalero,[45] F. M. Manganella,[37] D. Manuzzi,[25] D. Marangotto,[30,l] J. F. Marchand,[10] R. Marchevski,[50] U. Marconi,[25] E. Mariani,[16] S. Mariani,[49] C. Marin Benito,[45] J. Marks,[22] A. M. Marshall,[55] L. Martel,[64] G. Martelli,[34] G. Martellotti,[36] L. Martinazzoli,[49] M. Martinelli,[31,c] D. Martinez Gomez,[81] D. Martinez Santos,[84] F. Martinez Vidal,[48] A. Martorell i Granollers,[46] A. Massafferri,[2] R. Matev,[49] A. Mathad,[49] V. Matiunin,[44] C. Matteuzzi,[69] K. R. Mattioli,[15] A. Mauri,[62] E. Maurice,[15] J. Mauricio,[45] P. Mayencourt,[50] J. Mazorra de Cos,[48] M. Mazurek,[42] M. McCann,[62] T. H. McGrath,[63] N. T. McHugh,[60] A. McNab,[63] R. McNulty,[23] B. Meadows,[66] G. Meier,[19] D. Melnychuk,[42] D. Mendoza Granada,[16] P. Menendez Valdes Perez,[47] F. M. Meng,[4,m] M. Merk,[38,82] A. Merli,[50,30] L. Meyer Garcia,[67] D. Miao,[5,7] H. Miao,[7] M. Mikhasenko,[78] D. A. Milanes,[77,x] A. Minotti,[31,c] E. Minucci,[28] T. Miralles,[11] B. Mitreska,[19] D. S. Mitzel,[19] R. Mocanu,[43] A. Modak,[58] L. Moeser,[19] R. D. Moise,[17] E. F. Molina Cardenas,[87] T. Mombächer,[49] M. Monk,[57,1] S. Monteil,[11] A. Morcillo Gomez,[47] G. Morello,[28] M. J. Morello,[35,k] M. P. Morgenthaler,[22] A. Moro,[31,c] J. Moron,[40] W. Morren,[38] A. B. Morris,[49] A. G. Morris,[13] R. Mountain,[69] H. Mu,[4,m] Z. M. Mu,[6] E. Muhammad,[57] F. Muheim,[59] M. Mulder,[81] K. Müller,[51] F. Muñoz-Rojas,[9] R. Murta,[62] V. Mytrochenko,[52] P. Naik,[61] T. Nakada,[50] R. Nandakumar,[58] T. Nanut,[49] I. Nasteva,[3] M. Needham,[59] E. Nekrasova,[44] N. Neri,[30,l] S. Neubert,[18] N. Neufeld,[49] P. Neustroev,[44] J. Nicolini,[49] D. Nicotra,[82] E. M. Niel,[15] N. Nikitin,[44] L. Nisi,[19] Q. Niu,[74] P. Nogarolli,[3] P. Nogga,[18] C. Normand,[55] J. Novoa Fernandez,[47] G. Nowak,[66] C. Nunez,[87] H. N. Nur,[60] A. Oblakowska-Mucha,[40] V. Obraztsov,[44] T. Oeser,[17] A. Okhotnikov,[44] O. Okhrimenko,[53] R. Oldeman,[32,o] F. Oliva,[59,49] E. Olivart Pino,[45] M. Olocco,[19] C. J. G. Onderwater,[82] R. H. O'Neil,[49] J. S. Ordonez Soto,[11] D. Osthues,[19] J. M. Otalora Goicochea,[3] P. Owen,[51] A. Oyanguren,[48] O. Ozcelik,[49] F. Paciolla,[35,y] A. Padee,[42] K. O. Padeken,[18] B. Pagare,[47] T. Pajero,[49] A. Palano,[24] L. Palini,[30] M. Palutan,[28] C. Pan,[75] X. Pan,[4,m] S. Panebianco,[12] G. Panshin,[5] L. Paolucci,[63] A. Papanestis,[58] M. Pappagallo,[24,q] L. L. Pappalardo,[26] C. Pappenheimer,[66] C. Parkes,[63] D. Parmar,[78] B. Passalacqua,[26,g] G. Passaleva,[27] D. Passaro,[35,49,k] A. Pastore,[24] M. Patel,[62] J. Patoc,[64] C. Patrignani,[25,i] A. Paul,[69] C. J. Pawley,[82] A. Pellegrino,[38] J. Peng,[5,7] X. Peng,[74] M. Pepe Altarelli,[28] S. Perazzini,[25] D. Pereima,[44] H. Pereira Da Costa,[68] M. Pereira Martinez,[47] A. Pereiro Castro,[47] C. Perez,[46] P. Perret,[11] A. Perrevoort,[81] A. Perro,[49,13] M. J. Peters,[66] K. Petridis,[55] A. Petrolini,[29,j] S. Pezzulo,[29,j] J. P. Pfaller,[66] H. Pham,[69] L. Pica,[35,k] M. Piccini,[34] L. Piccolo,[32] B. Pietrzyk,[10] G. Pietrzyk,[14] R. N. Pilato,[61] D. Pinci,[36] F. Pisani,[49] M. Pizzichemi,[31,49,c] V. M. Placinta,[43] M. Plo Casasus,[47] T. Poeschl,[49] F. Polci,[16] M. Poli Lener,[28] A. Poluektov,[13] N. Polukhina,[44] I. Polyakov,[63] E. Polycarpo,[3] S. Ponce,[49] D. Popov,[7,49] S. Poslavskii,[44] K. Prasanth,[59] C. Prouve,[84] D. Provenzano,[32,49,o] V. Pugatch,[53] G. Punzi,[35,t] J. R. Pybus,[68] S. Qasim,[51] Q. Q. Qian,[6] W. Qian,[7] N. Qin,[4,m] S. Qu,[4,m] R. Quagliani,[49] R. I. Rabadan Trejo,[57] R. Racz,[80] J. H. Rademacker,[55] M. Rama,[35] M. Ramírez García,[87] V. Ramos De Oliveira,[70] M. Ramos Pernas,[57] M. S. Rangel,[3] F. Ratnikov,[44] G. Raven,[39] M. Rebollo De Miguel,[48] F. Redi,[30,w] J. Reich,[55] F. Reiss,[20] Z. Ren,[7] P. K. Resmi,[64] M. Ribalda Galvez,[45] R. Ribatti,[50] G. Ricart,[15,12] D. Riccardi,[35,k] S. Ricciardi,[58] K. Richardson,[65] M. Richardson-Slipper,[56] K. Rinnert,[61] P. Robbe,[14,49] G. Robertson,[60] E. Rodrigues,[61] A. Rodriguez Alvarez,[45] E. Rodriguez Fernandez,[47] J. A. Rodriguez Lopez,[77] E. Rodriguez Rodriguez,[49] J. Roensch,[19] A. Rogachev,[44] A. Rogovskiy,[58] D. L. Rolf,[19] P. Roloff,[49] V. Romanovskiy,[66] A. Romero Vidal,[47] G. Romolini,[26,49] F. Ronchetti,[50] T. Rong,[6] M. Rotondo,[28] S. R. Roy,[22] M. S. Rudolph,[69] M. Ruiz Diaz,[22] R. A. Ruiz Fernandez,[47] J. Ruiz Vidal,[82] J. J. Saavedra-Arias,[9] J. J. Saborido Silva,[47] S. E. R. Sacha Emile R.,[49] N. Sagidova,[44] D. Sahoo,[79] N. Sahoo,[54] B. Saitta,[32,o] M. Salomoni,[31,49,c] I. Sanderswood,[48] R. Santacesaria,[36] C. Santamarina Rios,[47] M. Santimaria,[28] L. Santoro,[2]

E. Santovetti,[37] A. Saputi,[26,49] D. Saranin,[44] A. Sarnatskiy,[81] G. Sarpis,[49] M. Sarpis,[80] C. Satriano,[36,z] M. Saur,[74] D. Savrina,[44] H. Sazak,[17] F. Sborzacchi,[49,28] A. Scarabotto,[19] S. Schael,[17] S. Scherl,[61] M. Schiller,[22] H. Schindler,[49] M. Schmelling,[21] B. Schmidt,[49] N. Schmidt,[68] S. Schmitt,[65] H. Schmitz,[18] O. Schneider,[50] A. Schopper,[62] N. Schulte,[19] M. H. Schune,[14] G. Schwering,[17] B. Sciascia,[28] A. Sciuccati,[49] G. Scriven,[82] I. Segal,[78] S. Sellam,[47] A. Semennikov,[44] T. Senger,[51] M. Senghi Soares,[39] A. Sergi,[29,49,j] N. Serra,[51] L. Sestini,[27] A. Seuthe,[19] B. Sevilla Sanjuan,[46] Y. Shang,[6] D. M. Shangase,[87] M. Shapkin,[44] R. S. Sharma,[69] I. Shchemerov,[44] L. Shchutska,[50] T. Shears,[61] L. Shekhtman,[44] Z. Shen,[38] S. Sheng,[5,7] V. Shevchenko,[44] B. Shi,[7] Q. Shi,[7] W. S. Shi,[73] Y. Shimizu,[14] E. Shmanin,[25] R. Shorkin,[44] J. D. Shupperd,[69] R. Silva Coutinho,[2] G. Simi,[33,v] S. Simone,[24,q] M. Singha,[79] N. Skidmore,[57] T. Skwarnicki,[69] M. W. Slater,[54] E. Smith,[65] K. Smith,[68] M. Smith,[62] L. Soares Lavra,[59] M. D. Sokoloff,[66] F. J. P. Soler,[60] A. Solomin,[55] A. Solovev,[44] K. Solovieva,[20] N. S. Sommerfeld,[18] R. Song,[1] Y. Song,[50] Y. Song,[4,m] Y. S. Song,[6] F. L. Souza De Almeida,[69] B. Souza De Paula,[3] K. M. Sowa,[40] E. Spadaro Norella,[29,j] E. Spedicato,[25] J. G. Speer,[19] P. Spradlin,[60] V. Sriskaran,[49] F. Stagni,[49] M. Stahl,[78] S. Stahl,[49] S. Stanislaus,[64] M. Stefaniak,[88] E. N. Stein,[49] O. Steinkamp,[51] H. Stevens,[19] D. Strekalina,[44] Y. Su,[7] F. Suljik,[64] J. Sun,[32] J. Sun,[63] L. Sun,[75] D. Sundfeld,[2] W. Sutcliffe,[51] V. Svintozelskyi,[48] K. Swientek,[40] F. Swystun,[56] A. Szabelski,[42] T. Szumlak,[40] Y. Tan,[4,m] Y. Tang,[75] Y. T. Tang,[7] M. D. Tat,[22] J. A. Teijeiro Jimenez,[47] A. Terentev,[44] F. Terzuoli,[35,y] F. Teubert,[49] E. Thomas,[49] D. J. D. Thompson,[54] A. R. Thomson-Strong,[59] H. Tilquin,[62] V. Tisserand,[11] S. T'Jampens,[10] M. Tobin,[5] T. T. Todorov,[20] L. Tomassetti,[26,g] G. Tonani,[30] X. Tong,[6] T. Tork,[30] D. Torres Machado,[2] L. Toscano,[19] D. Y. Tou,[4,m] C. Trippl,[46] G. Tuci,[22] N. Tuning,[38] L. H. Uecker,[22] A. Ukleja,[40] D. J. Unverzagt,[22] A. Upadhyay,[49] B. Urbach,[59] A. Usachov,[39] A. Ustyuzhanin,[44] U. Uwer,[22] V. Vagnoni,[25] V. Valcarce Cadenas,[47] G. Valenti,[25] N. Valls Canudas,[49] J. van Eldik,[49] H. Van Hecke,[68] E. van Herwijnen,[62] C. B. Van Hulse,[47,aa] R. Van Laak,[50] M. van Veghel,[38] G. Vasquez,[51] R. Vazquez Gomez,[45] P. Vazquez Regueiro,[47] C. Vázquez Sierra,[84] S. Vecchi,[26] J. Velilla Serna,[48] J. J. Velthuis,[55] M. Veltri,[27,bb] A. Venkateswaran,[50] M. Verdoglia,[32] M. Vesterinen,[57] W. Vetens,[69] D. Vico Benet,[64] P. Vidrier Villalba,[45] M. Vieites Diaz,[47,49] X. Vilasis-Cardona,[46] E. Vilella Figueras,[61] A. Villa,[25] P. Vincent,[16] B. Vivacqua,[3] F. C. Volle,[54] D. vom Bruch,[13] N. Voropaev,[44] K. Vos,[82] C. Vrahas,[59] J. Wagner,[19] J. Walsh,[35] E. J. Walton,[1,57] G. Wan,[6] A. Wang,[7] B. Wang,[5] C. Wang,[22] G. Wang,[8] H. Wang,[74] J. Wang,[6] J. Wang,[5] J. Wang,[4,m] J. Wang,[75] M. Wang,[49] N. W. Wang,[7] R. Wang,[55] X. Wang,[8] X. Wang,[73] X. W. Wang,[62] Y. Wang,[76] Y. Wang,[6] Y. H. Wang,[74] Z. Wang,[14] Z. Wang,[30] J. A. Ward,[57] M. Waterlaat,[49] N. K. Watson,[54] D. Websdale,[62] Y. Wei,[6] Z. Weida,[7] J. Wendel,[84] B. D. C. Westhenry,[55] C. White,[56] M. Whitehead,[60] E. Whiter,[54] A. R. Wiederhold,[63] D. Wiedner,[19] M. A. Wiegertjes,[38] C. Wild,[64] G. Wilkinson,[64,49] M. K. Wilkinson,[66] M. Williams,[65] M. J. Williams,[49] M. R. J. Williams,[59] R. Williams,[56] S. Williams,[55] Z. Williams,[55] F. F. Wilson,[58] M. Winn,[12] W. Wislicki,[42] M. Witek,[41] L. Witola,[19] T. Wolf,[22] E. Wood,[56] G. Wormser,[14] S. A. Wotton,[56] H. Wu,[69] J. Wu,[8] X. Wu,[75] Y. Wu,[6,56] Z. Wu,[7] K. Wyllie,[49] S. Xian,[73] Z. Xiang,[5] Y. Xie,[8] T. X. Xing,[30] A. Xu,[35,k] L. Xu,[4,m] L. Xu,[4,m] M. Xu,[49] Z. Xu,[49] Z. Xu,[7] Z. Xu,[5] K. Yang,[62] X. Yang,[6] Y. Yang,[15] Z. Yang,[6] V. Yeroshenko,[14] H. Yeung,[63] H. Yin,[8] X. Yin,[7] C. Y. Yu,[6] J. Yu,[72] X. Yuan,[5] Y Yuan,[5,7] E. Zaffaroni,[50] J. A. Zamora Saa,[71] M. Zavertyaev,[21] M. Zdybal,[41] F. Zenesini,[25] C. Zeng,[5,7] M. Zeng,[4,m] C. Zhang,[6] D. Zhang,[8] J. Zhang,[7] L. Zhang,[4,m] R. Zhang,[8] S. Zhang,[72] S. Zhang,[64] Y. Zhang,[6] Y. Z. Zhang,[4,m] Z. Zhang,[4,m] Y. Zhao,[22] A. Zhelezov,[22] S. Z. Zheng,[6] X. Z. Zheng,[4,m] Y. Zheng,[7] T. Zhou,[6] X. Zhou,[8] Y. Zhou,[7] V. Zhovkovska,[57] L. Z. Zhu,[7] X. Zhu,[4,m] X. Zhu,[8] Y. Zhu,[17] V. Zhukov,[17] J. Zhuo,[48] Q. Zou,[5,7] D. Zuliani,[33,v] and G. Zunica[28]

(LHCb Collaboration)

[1]*School of Physics and Astronomy, Monash University, Melbourne, Australia*
[2]*Centro Brasileiro de Pesquisas Físicas (CBPF), Rio de Janeiro, Brazil*
[3]*Universidade Federal do Rio de Janeiro (UFRJ), Rio de Janeiro, Brazil*
[4]*Department of Engineering Physics, Tsinghua University, Beijing, China*
[5]*Institute Of High Energy Physics (IHEP), Beijing, China*

[6]*School of Physics State Key Laboratory of Nuclear Physics and Technology, Peking University, Beijing, China*
[7]*University of Chinese Academy of Sciences, Beijing, China*
[8]*Institute of Particle Physics, Central China Normal University, Wuhan, Hubei, China*
[9]*Consejo Nacional de Rectores (CONARE), San Jose, Costa Rica*
[10]*Université Savoie Mont Blanc, CNRS, IN2P3-LAPP, Annecy, France*
[11]*Université Clermont Auvergne, CNRS/IN2P3, LPC, Clermont-Ferrand, France*
[12]*Université Paris-Saclay, Centre d'Etudes de Saclay (CEA), IRFU, Saclay, France, Gif-Sur-Yvette, France*
[13]*Aix Marseille Univ, CNRS/IN2P3, CPPM, Marseille, France*
[14]*Université Paris-Saclay, CNRS/IN2P3, IJCLab, Orsay, France*
[15]*Laboratoire Leprince-Ringuet, CNRS/IN2P3, Ecole Polytechnique, Institut Polytechnique de Paris, Palaiseau, France*
[16]*LPNHE, Sorbonne Université, Paris Diderot Sorbonne Paris Cité, CNRS/IN2P3, Paris, France*
[17]*I. Physikalisches Institut, RWTH Aachen University, Aachen, Germany*
[18]*Universität Bonn—Helmholtz-Institut für Strahlen und Kernphysik, Bonn, Germany*
[19]*Fakultät Physik, Technische Universität Dortmund, Dortmund, Germany*
[20]*Physikalisches Institut, Albert-Ludwigs-Universität Freiburg, Freiburg, Germany*
[21]*Max-Planck-Institut für Kernphysik (MPIK), Heidelberg, Germany*
[22]*Physikalisches Institut, Ruprecht-Karls-Universität Heidelberg, Heidelberg, Germany*
[23]*School of Physics, University College Dublin, Dublin, Ireland*
[24]*INFN Sezione di Bari, Bari, Italy*
[25]*INFN Sezione di Bologna, Bologna, Italy*
[26]*INFN Sezione di Ferrara, Ferrara, Italy*
[27]*INFN Sezione di Firenze, Firenze, Italy*
[28]*INFN Laboratori Nazionali di Frascati, Frascati, Italy*
[29]*INFN Sezione di Genova, Genova, Italy*
[30]*INFN Sezione di Milano, Milano, Italy*
[31]*INFN Sezione di Milano-Bicocca, Milano, Italy*
[32]*INFN Sezione di Cagliari, Monserrato, Italy*
[33]*INFN Sezione di Padova, Padova, Italy*
[34]*INFN Sezione di Perugia, Perugia, Italy*
[35]*INFN Sezione di Pisa, Pisa, Italy*
[36]*INFN Sezione di Roma La Sapienza, Roma, Italy*
[37]*INFN Sezione di Roma Tor Vergata, Roma, Italy*
[38]*Nikhef National Institute for Subatomic Physics, Amsterdam, Netherlands*
[39]*Nikhef National Institute for Subatomic Physics and VU University Amsterdam, Amsterdam, Netherlands*
[40]*AGH—University of Krakow, Faculty of Physics and Applied Computer Science, Kraków, Poland*
[41]*Henryk Niewodniczanski Institute of Nuclear Physics Polish Academy of Sciences, Kraków, Poland*
[42]*National Center for Nuclear Research (NCBJ), Warsaw, Poland*
[43]*Horia Hulubei National Institute of Physics and Nuclear Engineering, Bucharest-Magurele, Romania*
[44]*Authors affiliated with an institute formerly covered by a cooperation agreement with CERN*
[45]*ICCUB, Universitat de Barcelona, Barcelona, Spain*
[46]*La Salle, Universitat Ramon Llull, Barcelona, Spain*
[47]*Instituto Galego de Física de Altas Enerxías (IGFAE), Universidade de Santiago de Compostela, Santiago de Compostela, Spain*
[48]*Instituto de Fisica Corpuscular, Centro Mixto Universidad de Valencia—CSIC, Valencia, Spain*
[49]*European Organization for Nuclear Research (CERN), Geneva, Switzerland*
[50]*Institute of Physics, Ecole Polytechnique Fédérale de Lausanne (EPFL), Lausanne, Switzerland*
[51]*Physik-Institut, Universität Zürich, Zürich, Switzerland*
[52]*NSC Kharkiv Institute of Physics and Technology (NSC KIPT), Kharkiv, Ukraine*
[53]*Institute for Nuclear Research of the National Academy of Sciences (KINR), Kyiv, Ukraine*
[54]*School of Physics and Astronomy, University of Birmingham, Birmingham, United Kingdom*
[55]*H.H. Wills Physics Laboratory, University of Bristol, Bristol, United Kingdom*
[56]*Cavendish Laboratory, University of Cambridge, Cambridge, United Kingdom*
[57]*Department of Physics, University of Warwick, Coventry, United Kingdom*
[58]*STFC Rutherford Appleton Laboratory, Didcot, United Kingdom*
[59]*School of Physics and Astronomy, University of Edinburgh, Edinburgh, United Kingdom*
[60]*School of Physics and Astronomy, University of Glasgow, Glasgow, United Kingdom*
[61]*Oliver Lodge Laboratory, University of Liverpool, Liverpool, United Kingdom*
[62]*Imperial College London, London, United Kingdom*
[63]*Department of Physics and Astronomy, University of Manchester, Manchester, United Kingdom*
[64]*Department of Physics, University of Oxford, Oxford, United Kingdom*
[65]*Massachusetts Institute of Technology, Cambridge, Massachusetts, USA*

[66]University of Cincinnati, Cincinnati, Ohio, USA
[67]University of Maryland, College Park, Maryland, USA
[68]Los Alamos National Laboratory (LANL), Los Alamos, New Mexico, USA
[69]Syracuse University, Syracuse, New York, USA
[70]Pontifícia Universidade Católica do Rio de Janeiro (PUC-Rio), Rio de Janeiro, Brazil (associated with Universidade Federal do Rio de Janeiro (UFRJ), Rio de Janeiro, Brazil)
[71]Universidad Andres Bello, Santiago, Chile (associated with Physik-Institut, Universität Zürich, Zürich, Switzerland)
[72]School of Physics and Electronics, Hunan University, Changsha City, China (associated with Institute of Particle Physics, Central China Normal University, Wuhan, Hubei, China)
[73]Guangdong Provincial Key Laboratory of Nuclear Science, Guangdong-Hong Kong Joint Laboratory of Quantum Matter, Institute of Quantum Matter, South China Normal University, Guangzhou, China (associated with Department of Engineering Physics, Tsinghua University, Beijing, China)
[74]Lanzhou University, Lanzhou, China (associated with Institute Of High Energy Physics (IHEP), Beijing, China)
[75]School of Physics and Technology, Wuhan University, Wuhan, China (associated with Department of Engineering Physics, Tsinghua University, Beijing, China)
[76]Henan Normal University, Xinxiang, China (associated with Institute of Particle Physics, Central China Normal University, Wuhan, Hubei, China)
[77]Departamento de Fisica, Universidad Nacional de Colombia, Bogota, Colombia (associated with LPNHE, Sorbonne Université, Paris Diderot Sorbonne Paris Cité, CNRS/IN2P3, Paris, France)
[78]Ruhr Universitaet Bochum, Fakultaet für Physik und Astronomie, Bochum, Germany (associated with Fakultät Physik, Technische Universität Dortmund, Dortmund, Germany)
[79]Eotvos Lorand University, Budapest, Hungary (associated with European Organization for Nuclear Research (CERN), Geneva, Switzerland)
[80]Faculty of Physics, Vilnius University, Vilnius, Lithuania (associated with Physikalisches Institut, Albert-Ludwigs-Universität Freiburg, Freiburg, Germany)
[81]Van Swinderen Institute, University of Groningen, Groningen, Netherlands (associated with Nikhef National Institute for Subatomic Physics, Amsterdam, Netherlands)
[82]Universiteit Maastricht, Maastricht, Netherlands (associated with Nikhef National Institute for Subatomic Physics, Amsterdam, Netherlands)
[83]Tadeusz Kosciuszko Cracow University of Technology, Cracow, Poland (associated with Henryk Niewodniczanski Institute of Nuclear Physics Polish Academy of Sciences, Kraków, Poland)
[84]Universidade da Coruña, A Coruña, Spain (associated with La Salle, Universitat Ramon Llull, Barcelona, Spain)
[85]Department of Physics and Astronomy, Uppsala University, Uppsala, Sweden (associated with School of Physics and Astronomy, University of Glasgow, Glasgow, United Kingdom)
[86]Taras Schevchenko University of Kyiv, Faculty of Physics, Kyiv, Ukraine (associated with Université Paris-Saclay, CNRS/IN2P3, IJCLab, Orsay, France)
[87]University of Michigan, Ann Arbor, Michigan, USA (associated with Syracuse University, Syracuse, New York, USA)
[88]Ohio State University, Columbus, Ohio, USA (associated with Los Alamos National Laboratory (LANL), Los Alamos, New Mexico, USA)

[a]Deceased.
[b]Also at Lamarr Institute for Machine Learning and Artificial Intelligence, Dortmund, Germany.
[c]Also at Università degli Studi di Milano-Bicocca, Milano, Italy.
[d]Also at Università di Roma Tor Vergata, Roma, Italy.
[e]Also at Università di Modena e Reggio Emilia, Modena, Italy.
[f]Also at Department of Physics and Astronomy, University of Victoria, Victoria, Canada.
[g]Also at Università di Ferrara, Ferrara, Italy.
[h]Also at Universidade Estadual de Campinas (UNICAMP), Campinas, Brazil.
[i]Also at Università di Bologna, Bologna, Italy.
[j]Also at Università di Genova, Genova, Italy.
[k]Also at Scuola Normale Superiore, Pisa, Italy.
[l]Also at Università degli Studi di Milano, Milano, Italy.
[m]Also at Center for High Energy Physics, Tsinghua University, Beijing, China.
[n]Also at Universidad Nacional Autónoma de Honduras, Tegucigalpa, Honduras.
[o]Also at Università di Cagliari, Cagliari, Italy.
[p]Also at Centro Federal de Educacão Tecnológica Celso Suckow da Fonseca, Rio De Janeiro, Brazil.
[q]Also at Università di Bari, Bari, Italy.
[r]Also at Università di Perugia, Perugia, Italy.
[s]Also at LIP6, Sorbonne Université, Paris, France.

[t]Also at Università di Pisa, Pisa, Italy.
[u]Also at Hangzhou Institute for Advanced Study, UCAS, Hangzhou, China.
[v]Also at Università di Padova, Padova, Italy.
[w]Also at Università di Bergamo, Bergamo, Italy.
[x]Also at Universidad de Ingeniería y Tecnología (UTEC), Lima, Peru.
[y]Also at Università di Siena, Siena, Italy.
[z]Also at Università della Basilicata, Potenza, Italy.
[aa]Also at Universidad de Alcalá, Alcalá de Henares, Spain.
[bb]Also at Università di Urbino, Urbino, Italy.